University of Bath

Alternative formats

If you require this document in an alternative format, please contact:
openaccess@bath.ac.uk

REVISION

9th November 2017

Electroanalysis in 2D-TiO₂ Nanosheet Hosts: Electrolyte and Selectivity Effects in Ferroceneboronic Acid – Saccharide Binding

Wulan Tri Wahyuni [1,2], Budi Riza Putra [1,2], Christian Harito [3], Dmitry V. Bavykin [3], Frank C. Walsh [3], Tony D. James [1], Gabriele Kociok-Köhn [1,4], and Frank Marken*[1]

[1] Depatment of Chemtsiry, University of Bath, Claverton Down, Bath BA2 7AY, UK

[2] Department of Chemistry, Faculty of Mathematics and Natural Sciences, Bogor Agricultural University, Bogor, West Java, Indonesia

[3] Energy Technology Research Group, Faculty of Engineering and the Environment, University of Southampton, SO17 1BJ, Southampton, UK

[4] Chemical Characterisation and Analysis Facility (CCAF), University of Bath, Bath BA2 7AY, UK

To be submitted to Electroanalysis (Special Issue for Professor Joseph Wang)

Proof to F. Marken (f.marken@bath.ac.uk)

Abstract

A 2D-TiO$_2$ nanosheet material (as a film deposit of approximately 1 μm thickness on glassy carbon) is employed to host ferroceneboronic acid receptor molecules. It is suggested that the negative surface charge on 2D-TiO$_2$ nanosheets allows weak binding of ferroceneboronic acid, which can then be employed to detect fluoride, glucose, or fructose. The nature of the aqueous electrolyte is shown to strongly affect the ferroceneboronic acid – host interaction. In the presence of di-sodium sulfate stable reversible voltammetric responses are observed. In the presence of fluoride loss of the ferroceneboronic acid occurs probably due to weakening of the boron-titanate interaction. For glucose and for fructose "bound" and "unbound" states of the ferroceneboronic acid are observed as long as fast square wave voltammetry is employed to capture the "bound" state before decomplexation can occur. It is shown that this kinetic selectivity is highly biassed towards fructose and essentially insensitive to glucose.
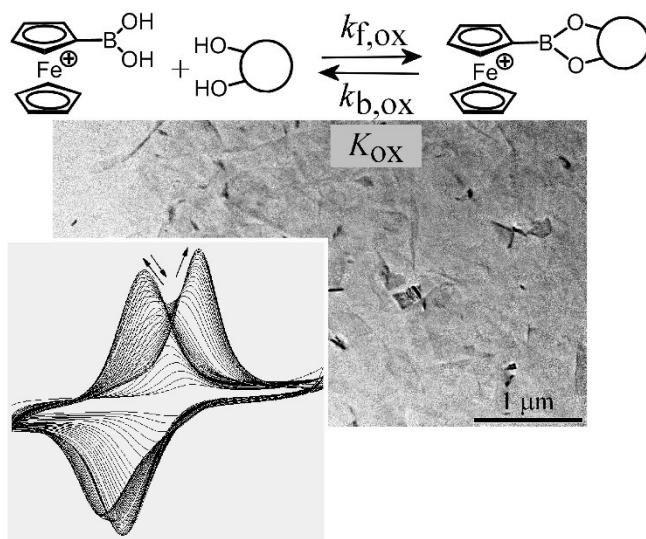
Graphical Abstract

Keywords: 2D-nanosheets; saccharide; double layer; lamella structure; release.

1. Introduction

New types of 2D nanooxide materials emerge as new synthetic approaches are developed. The pioneering work by Sasaki [1] introduced a 2D titanate materials obtained by two consecutive steps including (i) solid state high temperature reaction forming crystalline layered bulk cesium titanate, followed by (ii) ion exchange of cesium to quarternary ammonium cations accompanying delamination of single layered titanate nanosheets into aqueous solution. The thickness of these nanosheets corresponds to that of a single unit cell. The availability of 2D-nanooxides opens up a range of opportunities from energy storage to sensing. Applications for 2D-nanooxides (and related materials) have been suggested in electrocatalysis [2], as electronic components [3], and in membrane systems with ion selectivity [4]. Novel photoelectrochemcial systems based on 2D-nanooxide and lamella structures have been reported based on TiO_2 [5], Nb_3O_8 [6], ZnO [7], and based on $BiVO_4$ [8,9]. In particular 2D-$BiVO_4$ appears to attract attention [10]. Here, sensing with a 2D-nanooxide host based on single layered titanate is reported.

Nanostructured titanates or salts of poly-titanic acids can be synthesised in various shapes and morphologies such as tubular, fibours, spheroidal, or flat, and depending on their dimenstions, can be used in a wide range of applications [11]. Lepidocrocite nanosheets have been first developed by Sasaki's group [12,13]. The typical thickness of single layer nanosheet measured by AFM was reported as 1.2 – 1.3 nm [14]. The crystal structure of these sheets is approximated as $H_{0.7}Ti_{1.825}0_{0.175}O_4 \bullet H_2O$, where a cation is needed for every 0.38 Ti to stabilise the charged surface. Depending on the nature of stabilizing cation re-stacking nanosheets back into multilayered structures can be avoided or delayed. In previous work it has been shown that TiO_2 nanosheets can be highly beneficial as an additive to a polymer composite materials [15] imroving their mechanical properties. A report on potential applications of multi-layer TiO_2 nanosheet deposits in electroanalysis has appeared recently [16].

In this study, ferroceneboronic acid is investigated in conjunction with 2D-nanooxide based on titanates. Ferroceneboronic acid has been employed previously in a range of sensing applications

[17,18] due to the ability to bind to vicinal diols [19]. In a recent report it has been shown that voltammetric responses for ferroceneboronic acid in solution are affected by kinetic parameters [20] (and are not necessarily a reflection of only equilibrium concentrations). The electrochemical reaction path shown in Figure 1 is summarised as a square shape scheme for the Fe(III/II) redox process coupled to the saccharide binding to the boronic acid. The scheme is over-simplified with other species and intermediates potentially also being important. It was observed that the oxidised form, ferriceniumboronic acid, binds more strongly (to fructose) and when scanning the applied potential from more positive to negative the rapid release of the saccharide occurs. The rate constant $k_{b,ox}$ (when fast compared to the time constant of the detection method) allows the saccharide – ferroceneboronic acid complex to decay without being detected. It was concluded that only fast voltmmetric methods are suitable to detect the ferroceneboronic acid – saccharide complex. A similar obervation is reported here for the case of immobilised ferroceneboronic acid in a 2D-nanooxide host based on titanate.
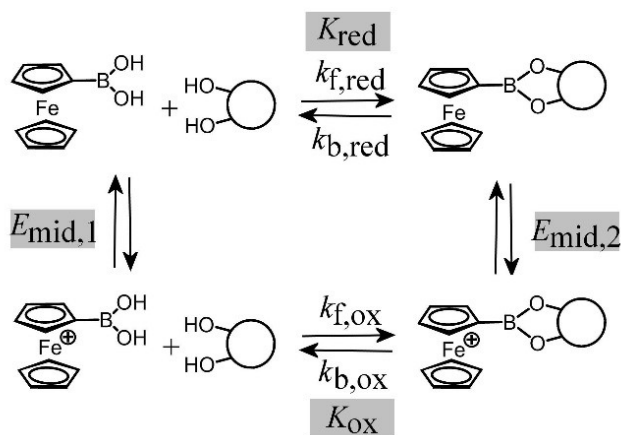
Figure 1. Schematic representation of the electrochemical square scheme based on ferrocene-boronic acid binding to a saccharide with two distinct electroactive species.

In this report, the immobilisation of ferroceneboronic acid is investigated into the lamella-structured film deposit formed from colloidal titanate nanosheet material by drop-casting onto a glassy carbon electrode. Ferroceneboronic acid can be immobilsied when working in aqueous

Na_2SO_4 and is released when interacting with fluoride, glucose, or fructose. For fructose the ferroceneboronic acid complex is detected over a 5 to 100 mM concentration range.

2. Experimental

2.1. Chemical Reagents

TiO_2 nanosheet material was synthesized as described previously by Sasaki [14] and by Harito et al. [15]. Ferrocene-boronic acid (molecular weight 229.85 g nol^{-1}; CAS: 12152-94-2; >98%) was purchased from Tokyo Chemical Industry Co., Ltd, sodium dihydrogen phosphate was used for buffer preparation (from Fisher Scientific), sodium chloride, sodium nitrate, sodium perchlorate, sodium sulfate, fructose, glucose, and sodium fluoride were obtained from Sigma–Aldrich or Fisher Scientific and used without further purification. Solutions were prepared under ambient condition in volumetric flash with ultrapure water with resistivity of 18.2 Mohm cm (at 22 $^{\circ}$C) from ELGA Purelab Classic system.

2.2. Instrumentation

Cyclic voltammetry was performed using a classic three-electrode system controlled with a microAutolab III system (Metrohm-Autolab, Netherlands) in normal voltammetry mode. The scan rate was maintained at 50 mV s^{-1}. The counter and reference electrodes, respectively, were platinum wire and KCl-saturated calomel (SCE). The working electrode was a 3.0 mm-diameter glassy carbon electrode (GCE) modified by TiO_2 nanosheet film. GCE was polished with alumina slurry and sonicated for 10 minute each in ethanol and water before modification with TiO_2 nanosheet films. Characterization of TiO_2 nanosheet ferroceneboronic acid composites was carried out using Scanning Electron Microscopy (JEOL SEM6480LV) and Transmission Electron Microscopy analysis (JEOL JEM-2100Plus). X-ray diffraction data (XRD) for an ambiently dried sample of the TiO_2 nanosheet materials were obtained on a Bruker AXS D8 Advance diffractometer with a θ–2θ configuration and using CuKα radiation λ=1.5418 Å).

2.3. Preparation of the Working Electrode

Procedure 1 (without ferroceneboronic acid): An aliquot of 5 µL TiO$_2$ nanosheet colloidal solution (2.56 g L^{-1}) was deposited on to GCE surface by drop casting method without addition of any binding materials. The solution was was dried at ambient temperature forming a transparent thin film of titanate nanosheets (see below) prior to use.

Procedure 2 (with ferroceneboronic acid): TiO$_2$ nanosheet colloidal solution (2.56 g L^{-1}) and ferrocene boronic acid (1 mM in water or 230 mg L^{-1}) were mixed in ratio of (10:1) by volume. An aliquot of 5 µL TiO$_2$ nanosheet:ferrocene boronic acid mixture was then deposited onto the GCE surface by drop casting method. The film was dried at ambient temperature prior to use.

3. Results and Discussion

3.1. Characterisation of TiO$_2$ Nanosheet Ferroceneboronic Acid Composites

Titanate nanosheet materials were obtained following the method developed by Sasaki et al. [21], which is based on two steps process involving (i) calcination of bulk TiO$_2$ with Cs$_2$CO$_3$ followed by ion exchange Cs$^+$ to H$^+$; and then (ii) exfoliation of titanate nanosheets in the presence of triethylamin at room temperature forming stable colloidal solution [15]. A colloidal solution of typically 2.56 g L^{-1} titanate nanosheets is obtained and employed here for modification of electrodes. Figure 2A shows transmission electron microscopy (TEM) images of the nanosheets as individual superimposed sheets, which are typically one unit cell thick and typically 1 µm in lateral size. Films are readily obtained by drop casting of the colloidal solution onto glassy carbon electrodes. Thin uniform films can be seen with the help of scanning electron microscopy (SEM). When scratching the film with a scalpel (see Figure 2B) the thickness of deposits can be estimated as typically 1 µm.
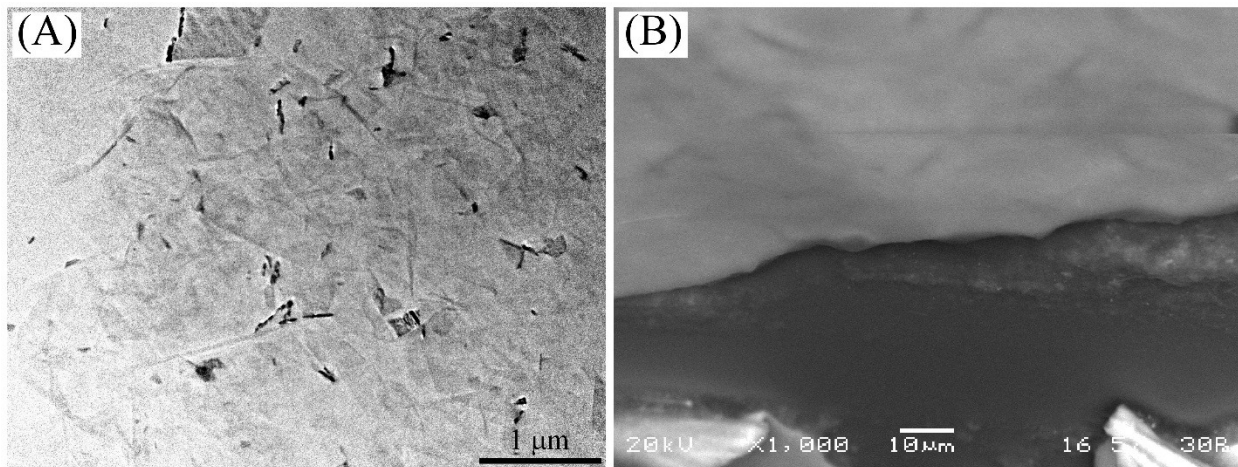
Figure 2. (A) Transmission electron micrograph (TEM) of TiO$_2$ nanosheet material. (B) Scanning electron micrograph (SEM) of a film of TiO$_2$ nanosheet material deposited onto glassy carbon and scratched with a scalpel to reveal the cross section.

In order to explore the packing of TiO$_2$ nanosheet films X-ray diffraction (XRD) pattern were measured for film deposits on a silicon substrate. Figure 3 shows diffraction data for (A) the pure TiO$_2$ nanosheet colloid and (B) the TiO$_2$ nanosheet solution with ferrroceneboronic acid in 111:1 weight ratio (see experimental) or approximately 320 : 1 Ti : Fe atomic ratio. The ferroceneboronic acid is present at realtively low concentration and attempts to detect iron by energy-dispersive x-ray elemental analysis (EDX) failed. However, the presence of the ferroceneboronic acid is clearly revealed by a pale yellow coloration.
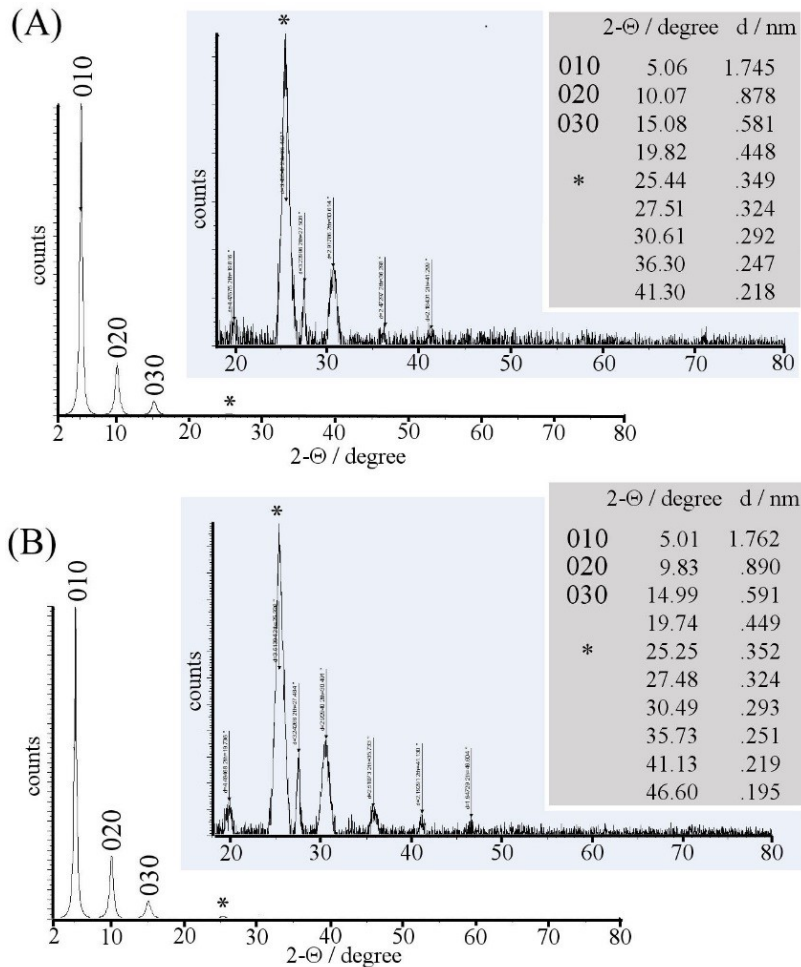
Figure 3. XRD pattern for (A) TiO$_2$ nanosheets and (B) TiO$_2$ nanosheets with ferroceneboronic acid.

X-ray powder diffraction data were obtained and revealed the strong diffracting signals for 010, 020, and 030 peaks. This is consistent with literature reports and can be interpreted in terms of a layered structure with an average interlayer spacing of (A) 1.745 nm and (B) 1.762 nm. The actual thickness of individual TiO$_2$ nanosheet layers has been reported as 1.2 to 1.3 nm [14], but additional hydration and adsorbate layers need to be considered. The sample with added ferroceneboronic acid appears to exhibit only a slight widening of the inter-layer gap indicating intercalation of ferroceneboronic acid between the layers. Additional diffraction peaks are observed at higher angle but are currently not fully identified.

3.2. Electrochemistry of TiO₂ Nanosheet Ferroceneboronic Acid Composites: Electrolyte Effects

TiO$_2$ nanosheet materials, being protonated form of poly-titanate, are negatively charged at the surface and often stabilized with cationic species. Here, in addition to quaternary ammonium cations the Lewis acidic molecule ferroceneboronic acid is employed and an interaction from electrophilic boron to nucleophilic titanate is anticipated to lead to weak binding. This can be investigated with the help of cyclic voltammetry experiments. A film of TiO$_2$ nanosheets of approximately 1 μm thickness is applied to a glassy carbon electrode and then immersed into aqueous electrolyte solution containing 1 mM ferroceneboronic acid. Data in Figure 4A show (for 0.1 M phosphate buffer pH 7) the voltammetric response for ferroceneboronic acid developing at a potential of E_{mid} = 0.13 V vs. SCE (with E_{mid} = ½ E_{ox} + ½ E_{red}). The peak saturates at approximately 3.8 μA peak current (at a scan rate of 50 mV s^{-1}). The peak-to-peak separation for this oxidation-reduction process is approximately 30 mV, which is indicative for a surface-immobilised redox system. During the ferroceneboronic acid adsorption process a shift of the E_{mid} potential in negative direction occurs. When transferring this electrode into pure phosphate buffer solution without the ferroceneboronic acid, unfortunately the voltammetric response exhibits some decay and a splitting into two signals. The reason for peak potential shift and peak splitting may be linked in part to competing processes involving different types of cations/anions. A shift of the voltammetric to more negative potential would imply some stabilisation of the oxidized ferriceniumboronic acid state.
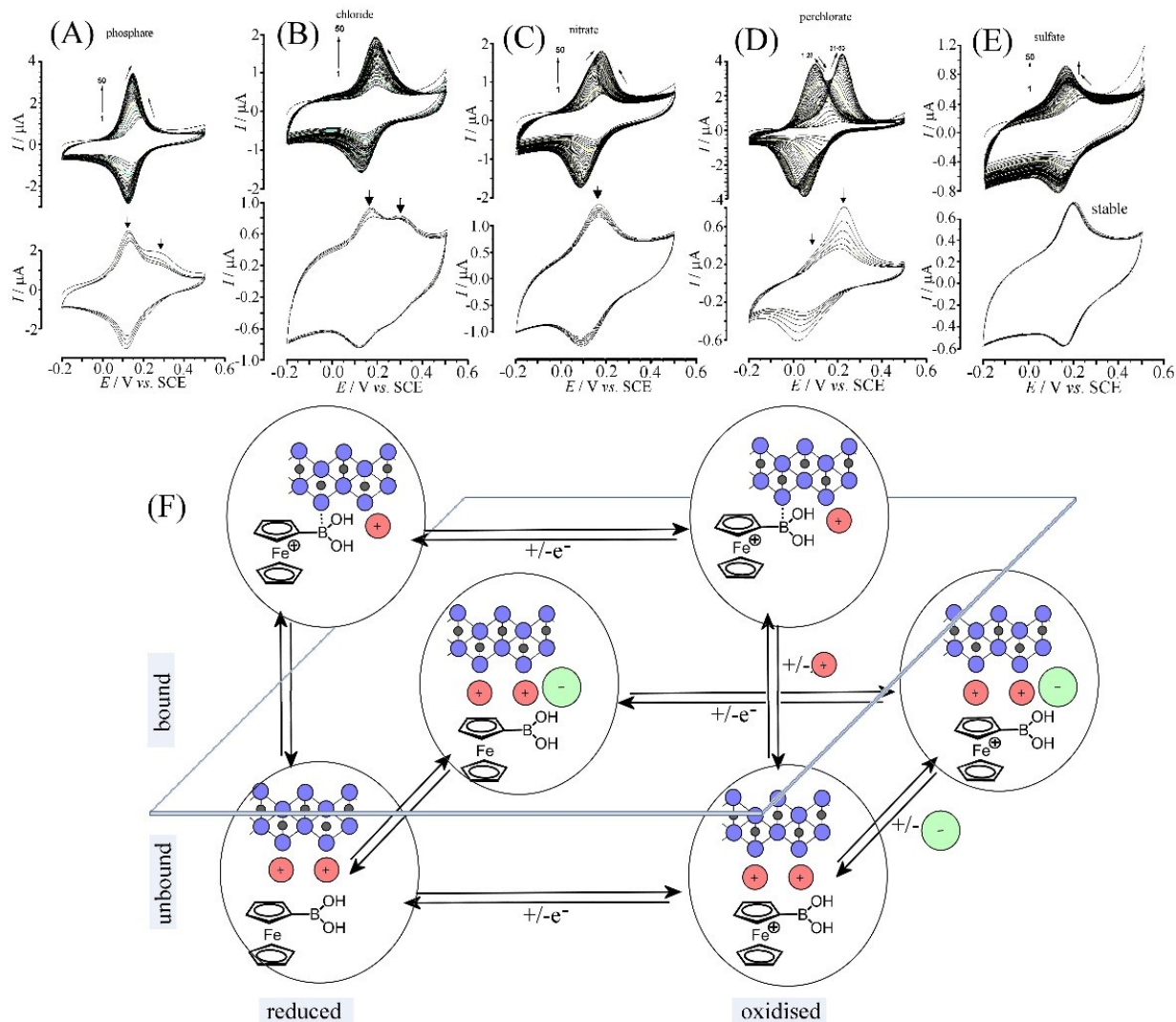
Figure 4. Cyclic voltammogram (50 continuous cycles; scan rate 50 mV s^{-1}) for GCE-TiO$_2$ nanosheet in (A) 0.1 M phosphate buffer pH 7, (B) 0.1 M NaCl, (C) 0.1 M NaNO$_3$, (D) 0.1 M NaClO$_4$, (E) 0.1 M Na$_2$SO$_4$ with in 1 mM of ferroceneboronic acid. Below is shown another set of 4-6 potential cycles after transfer into electrolytes solution without ferroceneboronic acid. (F) Schematic drawing of the interaction of ferroceneboronic acid during redox cycling with TiO$_2$ nanosheet and electrolyte.

The charge under the voltammetric oxidation/reduction peak responses is relatively low (typically 2-4 μC), which is indicative of only limited transport of charges (via hopping) within the lamella space of the 2D-TiO$_2$ nanosheet material deposit. Next, the electrolyte effect on electrochemistry of TiO$_2$ nanosheet ferroceneboronic acid composites was investigated. Further cyclic voltammetry experiments (50 continuous cycles; scan rate 50 mV s^{-1}) for the TiO$_2$ nanosheet modified electrode

was performed in 1 mM ferrocene-boronic acid solution and in different types of electrolytes (0.1 M phosphate buffer pH 7, 0.1 M NaCl, 0.1 M NaNO₃, 0.1 M NaClO₄, and 0.1 M Na₂SO₄). After 50 cyclic voltammetry experiments in 1 mM ferroceneboronic solution, the electrode was transferred to electrolyte without ferroceneboronic acid and investigated for stability (Figure 4). Data for chloride electrolyte (Figure 4B) suggests relatively simple behaviour during ferroceneboronic acid adsorption, but decay of the voltammetric response in the absence of ferroceneboronic acid. In the presence of nitrate (Figure 4C) a more complex behavior during ferroceneboronic acid binding occurs. Data for perchlorate (Figure 4D) seem particularly intriguing with build-up of an initial pair of peaks (peak-to-peak separation of 47 mV) followed by development of a second type of peak (peak-to-peak separation 230 mV). The widening of the peak-to-peak separation has to be assigned to two more chemically distinct states for Fe(II) and Fe(III) possibly associated with a binding process (electrolyte sensitive). In the scheme in Figure 4F this is indicated (hypothetically) as bound/unbound structures where the boron-titanate interaction is important. The interaction of the titanate with the boron would be expected to move electron density into the ferrocene and thereby shift the E_{mid} potential more negative. The effect of the electrolyte anion in these equilibria appears to be subtle and is currently not fully understood. In Figure 4F it is suggested that the electrolyte anion can affect the removal of the electrolyte cation from the titanate surface to indirectly affect binding to ferroceneboronic acid. The complexity in these equilibria currently prevents further quantitative insights. For the purpose of the current study achieving a stable voltammetric response is most important.

When investigating the case for Na₂SO₄ electrolyte (Figure 4E) the voltammetric response for the ferroceneboronic acid adsorption process appeared less complex and after transfer into electrolyte without ferroceneboronic acid the voltammetric response remained stable. Therefore in the presence of sulfate anions the interaction between ferroceneboronic acid and titanate surface appears more robust towards redox cycling and therefore more suitable for sensor application. Therefore the following experiments are performed in aqueous 0.1 M Na₂SO₄. Also, the preparation of the TiO₂ nanosheet ferroceneboronic acid composite modified electrode is simplified into a direct co-deposition with ferroceneboronic acid and TiO₂ in 1:111 weight ratio (see experimental).

3.3. Electrochemistry of TiO_2 Nanosheet Ferroceneboronic Acid Composites: Fructose Binding

It is well known that fructose can interact strongly with ferroceneboronic acid (in aqueous buffer solution) resulting in a shift of the Fe(III/II) potential negative by typically 0.18 V at pH 7. This shift is associated with fructose binding (see Figure 1). In order to investigated fructose binding aqueous 0.1 M Na_2SO_4 is selected and the electrode preparation is simplified. Figure 5A and 5B show cyclic voltammetry responses for the 50-cycle equilibrated electrode (5A) and an electrode simply modified with a TiO_2 nanosheet ferroceneboronic acid composite (see experimetnal). The composite electrode exhibits well-defiend voltammetric signals, which are stable and consistent with those observed in Figure 4E. Therefore the composite modificaiton mehtod is employed in the following experiments.

Fructose solutions at concentration of 25, 50, and 100 mM were prepared in 0.1 M Na_2SO_4 and the electrochemical behaviour of the TiO_2 nanosheet ferroceneboronic acid composite electrode was investigated in these fructose solutions. Figure 5C shows data for the equilibrated electrode and Figure 5D shows data for the TiO_2 nanosheet ferroceneboronic acid composite electrode. Both electrodes show similar behaviour with fructose causing (i) a decay of the current peaks and (ii) the appearance of a new current peak approximately 0.18 V more negative. This suggests that fructose can bind and weaken the interaction to titanate. As the result the decay of the voltammetric response is observed. The smaller more negative voltammetric signal is consistent with the fructose-ferroceneboronic acid complex (Figure 1).

Fluoride also is known to strongly bind to boronic acids and therefore additional measurements were performed with fluoride in 25 mM, 50 mM, and 100 mM concentration (Figure 5E). Again loss of the voltammetric signal is consistent with complex formation and loss of ferroceneboronic acid from the titanate film into the electrolyte solution. These experiemnts demonstrate that binding to ferroceneboronic acid within the TiO_2 nansheet matrix can be observed. In order to provide analytically more defined signals square wave voltammetric methods are employed next.
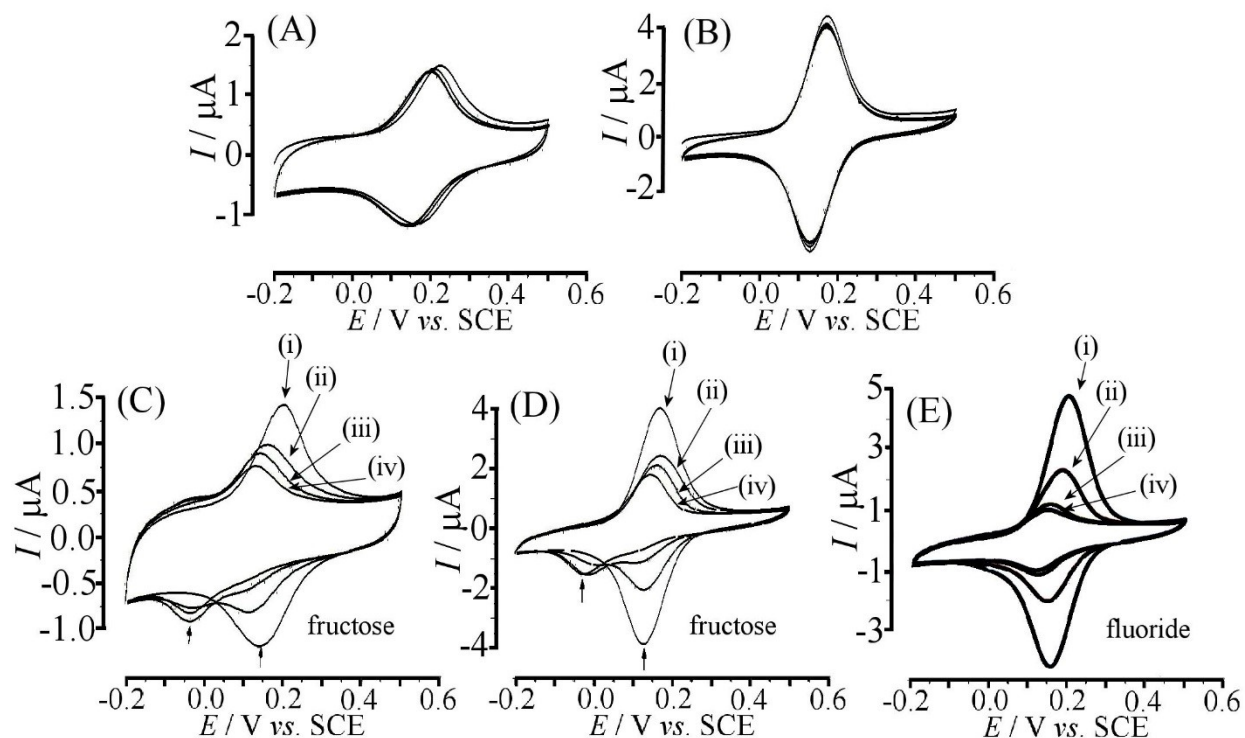
12

Figure 5. Cyclic voltammogram (four continuous cycles; scan rate 50 mV s^{-1}) in 0.1 M Na$_2$SO$_4$ for (A) a TiO$_2$ nanosheet composite electrode previously potential-cycled in 0.1 M Na$_2$SO$_4$ containing 1 mM ferroceneboronic acid and (B) a composite deposit of TiO$_2$ nanosheets and ferroceneboronic acid. (C) Cyclic voltammograms for electrode A after addition of 0, 25, 50, 100 mM fructose. (D) Cyclic voltammograms for electrode B after addition of 0, 25, 50, 100 mM fructose. (E) Cyclic voltammogram (scan rate 50 mV s^{-1}) for electrode B in 0.1 M Na$_2$SO$_4$ after addition of 0, 25, 50, 100 mM fluoride.

Figure 6 shows data from square wave voltammetry for TiO$_2$ nanosheet ferroceneboronic acid composite film electrodes immersed in 0.1 M Na$_2$SO$_4$ containing (i) 25, (ii) 50, and (iii) 100 mM fructose. In this case two clear peak signals are assocaited with the ferroceneboronic acid precursor (at 0.18 V vs. SCE) and the fructose complex (at 0.0 V vs. SCE). Consistent with a previuos study [16] the effect of scan rate can be exploited to increase the signal for the fructose complex. In

Figure 1 the oxidised form of ferrocene boronic acid causes stronger binding to fructose (reported for aqueous pH 7 buffer are $K_{ox} = 300$ M^{-1} and $K_{red} = 0.2$ M^{-1} [16], but these values may change in the TiO$_2$ nanosheet host). During the reduction the much weaker bound reduced form is generated. For the case of the scan rate being slow the situation arises that ferroceneboronic acid is converted to Fe(II) state and the fructose – ferroceneboronic acid complex is still in Fe(III) state. Therefore fructose decomplexation and reduction can occur and this causes loss of the current peak for the fructose – ferroceneboronic acid complex. In Figure 6A-C the effect of scan rate is clearly demonstrated. When studying scan rates of 41.5 mVs^{-1} (step potential 0.005 V), 83 mVs^{-1} (step potential 0.01 V), and 124.5 mVs^{-1} (step potential 0.015 V) only for the faster scan rate is the fructose complex clearly detected. Therefore the faster scan rate is selected for the quantitative analysis of fructose.
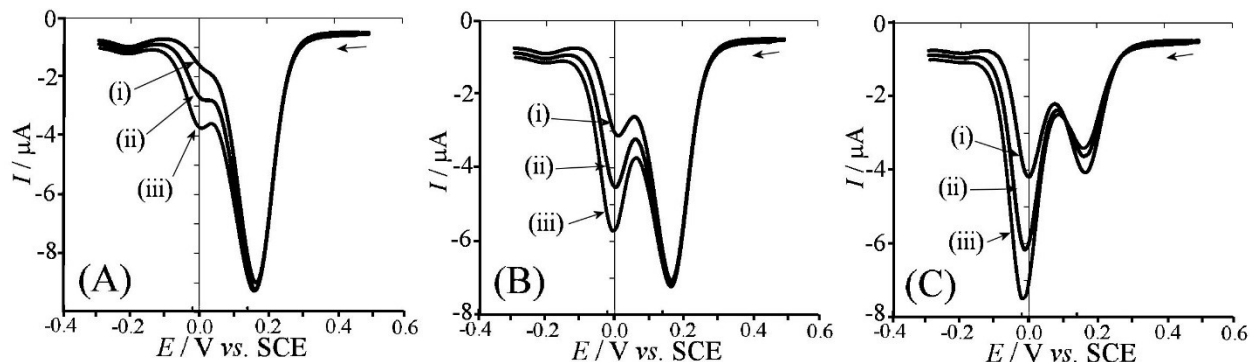

Figure 6. Square wave voltammograms for a TiO$_2$ nanosheet ferroceneboronic acid composite film electrode in 0.1 M Na$_2$SO$_4$ with (A) 25 mM, (B) 50 mM, (C) 100 mM fructose (scan rate (i) 41.5 mVs^{-1} (step potential 0.005 V), scan rate (ii) 83 mVs^{-1} (step potential 0.01 V), scan rate (iii) 124.5 mVs^{-1} (step potential 0.015 V).

Figure 7 shows square wave voltammetry data (scan rate of 124.5 mVs^{-1}) for the TiO$_2$ nanosheet ferroceneboronic acid composite electrodes immersed in 0.1 M Na$_2$SO$_4$ solution with Gaussian deconvolution of peaks. Data were obtained for a range of concentrations and for both fructose and glucose. The deconvolution process allows peak currents for bound and unbound to be distinguished and a plot of $I_{bound}/I_{unbound}$ versus concentration to be constructed. For glucose no

significant increase in the current for the bound state is observed relative to the current for the unbound state. In contrast a well-defined concentration dependence is observed for fructose in the concentration range 5 to 100 mM. The method is therefore highly sensitive to saccharide structure.
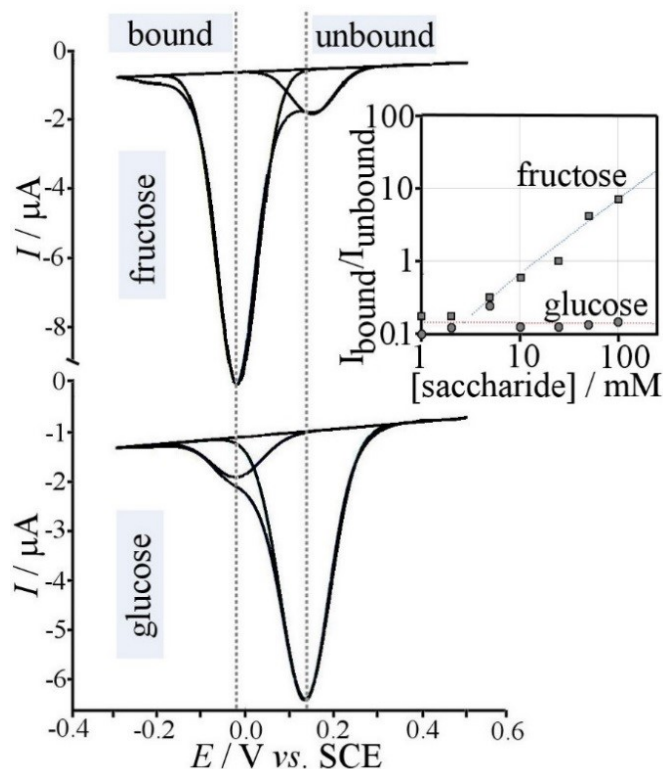

Figure 7. Square wave voltammograms (scan rate 124.5 mVs^{-1}; step potential 0.015 V) for a TiO$_2$ nanosheet ferroceneboronic acid composite film electrode in 0.1 M Na$_2$SO$_4$ with 100 mM fructose and with 100 mM glucose. Inset: plot of the peak current ratio I$_{bound}$/I$_{unbound}$ from convolution analysis *versus* saccharide concentration.

The ability to distinguish between saccharides is interesting, although the detection of glucose clearly would be of higher urgency. However, the fact that a high selectivity can be achieved is promising and this could be further investigated to induce better selectivity towards glucose by tuning of the molecular environment of the ferroceneboronic acid in the TiO$_2$ nanosheet composite. The effects of the TiO$_2$ nanosheets are likely to include (i) binding ferroceneboronic acid without loss of ability to interact with saccharides, (ii) changing selectivity and in particular enhancing

selectivity towards fructose, and (iii) avoiding effects from larger molecules (proteins, glycosylated or glycated proteins, poly-saccharides, etc.), which could interfere in more open sensor architectures with immobilized ferroceneboronic acid receptors.

4. Conclusions

It has been shown that ferroceneboronic acid can be bound into a matrix of lamella 2D-TiO_2 nanosheet material and deposited onto a glassy carbon working electrode in the form of an electro-active thin film. Stable voltammetric responses for Fe(II/III) are observed in aqueous 0.1 M Na_2SO_4 electrolyte, but more complex behavior (probably due to electrolyte salt affecting boronic acid – TiO_2-nanosheet interactions) is observed in other types of electrolyte media. Fluoride strongly/quickly removes the ferroceneboronic acid. Fructose and glucose in the electrolyte lead to voltammetric signals that correspond to a bound and an unbound state due to bidentate boronic acid complexation. Optimised conditions (taking into account kinetically controlled decomplexation of the ferroceneboronic acid) allow square wave voltammetry detection of fructose in a 2 mM to 100 mM concentration range even in the presence of glucose. More work will be required to optimise the analytical procedure and to establish limit of detection data for different saccharides. In the future, 2D-nanooxide environments could be employed as matrix for ferroceneboronic acid receptor molecules to work, for example in more complex biological media (e.g. in blood). The lamella structure is likely to suppress interaction with molecules of higher molecular weight and at the same time allows interaction with smaller saccharides such as fructose and glucose to be affected.

References

[1]   L. Wang and T. Sasaki, *Chem. Rev.*, **2014**, *114*, 9455–9486.

[2]   W. Zhang and K. Zhou, *Small*, **2017**, *13*, 1700806.

[3]   S. Kang, X. Mou, B. Fallahazad, N. Prasad, X. Wu, A. Valsaraj, H.C.P. Movva, K. Kim, E. Tutuc, L.F. Register and S.K. Banerjee, *J. Phys. D-Appl. Phys.*, **2017**, *50*, 383002.

[4]   J. Gao, Y.P. Feng, W. Guo and L. Jiang, *Chem. Soc. Rev.*, **2017**, *46*, 5400–5424.

[5]   N. Sakai, K. Kamanaka and T. Sasaki, *J. Phys. Chem. C*, **2016**, *120*, 23944–23950.

[6]   T. Shibata, G. Takanashi, T. Nakamura, K. Fukuda, Y. Ebina and T. Sasaki, *Energy Environm. Sci.*, **2011**, *4*, 535–542.

[7]   S. Singh, R. Sharma and B.R. Mehta, *Appl. Surface Sci.*, **2017**, *411*, 321–330.

[8]   J.Q. Li, D.F. Wang, H. Liu, J. Du and Z.F. Zhu, *Phys. Status Solidi A-Appl. Mater. Sci.*, **2012**, *209*, 248–253.

[9]   A.L. Wang, S. Shen, Y.B. Zhao and W. Wu, *J. Colloid. Interf. Sci.*, **2015**, *445*, 330–336.

[10]   Z.R. Tang, Q.Q. Yu and Y.J. Xu, *RSC Adv.*, **2014**, *4*, 58448–58452.

[11]   D.V. Bavykin, J.M. Friedrich and F.C. Walsh, *Adv. Mater.*, **2006**, *18*, 2807–2824.

[12]   T. Sasaki and M. Watanabe, *J. Phys. Chem. B*, **1997**, *101*, 10159–10161.

[13]   T. Sasaki, *Supramol. Sci.*, **1998**, *5*, 367–371.

[14]   T. Sasaki, Y. Ebina, Y. Kitami, M. Watanabe and T. Oikawa, *J. Phys. Chem. B*, **2001**, *105*, 6116–6121.

[15]   C. Harito, D.V. Bavykin, M.E. Light and F.C. Walsh, *Composites B*, **2017**, *124*, 54–63.

[16]   K. Ahmad, A. Mohammad, R. Rajak, and S.M. Mobin, *Mater. Res. Express*, **2016**, *3*, 074005.

[17]   M. Li, W.H. Zhu, F. Marken and T.D. James, *Chem. Commun.*, **2015**, *51*, 14562–14573.

[18]   B.Z. Wang, S. Takahashi, X.Y. Du, and J.I. Anzai, *Biosensors*, **2014**, *4*, 243–256.

[19]   E. Galbraith and T.D. James, *Chem. Soc. Rev.*, **2010**, *39*, 3831–3842.

[20]   M. Li, S.Y. Xu, A.J. Gross, J.L. Hammond, P. Estrela, J. Weber, K. Lacina, T.D. James and F. Marken, *ChemElectroChem*, **2015**, *2*, 867–871.

[21]   N. Sakai, Y. Ebina, K. Takada, T. Sasaki, *J. Am. Chem. Soc*, **2004**, *126*, 5851–5859.